# Characterization of Arabidopsis Lines Deficient in GAPC-1, a Cytosolic NAD-Dependent Glyceraldehyde-3-Phosphate Dehydrogenase[1][C]

**Sebastián P. Rius, Paula Casati, Alberto A. Iglesias, and Diego F. Gomez-Casati***

Instituto de Investigaciones Biotecnológicas-Instituto Tecnológico de Chascomús, CONICET/UNSAM, 7130, Chascomús, Argentina (S.P.R., D.F.G.-C.); Centro de Estudios Fotosintéticos y Bioquímicos, Universidad Nacional de Rosario, 2000, Rosario, Argentina (P.C.); and Laboratorio de Enzimología Molecular, Facultad de Bioquímica y Ciencias Biológicas, Universidad Nacional del Litoral, 3000, Santa Fe, Argentina (A.A.I.)

Phosphorylating glyceraldehyde-3-P dehydrogenase (GAPC-1) is a highly conserved cytosolic enzyme that catalyzes the conversion of glyceraldehyde-3-P to 1,3-bis-phosphoglycerate; besides its participation in glycolysis, it is thought to be involved in additional cellular functions. To reach an integrative view on the many roles played by this enzyme, we characterized a homozygous *gapc-1* null mutant and an *as-GAPC1* line of Arabidopsis (*Arabidopsis thaliana*). Both mutant plant lines show a delay in growth, morphological alterations in siliques, and low seed number. Embryo development was altered, showing abortions and empty embryonic sacs in basal and apical siliques, respectively. The *gapc-1* line shows a decrease in ATP levels and reduced respiratory rate. Furthermore, both lines exhibit a decrease in the expression and activity of aconitase and succinate dehydrogenase and reduced levels of pyruvate and several Krebs cycle intermediates, as well as increased reactive oxygen species levels. Transcriptome analysis of the *gapc-1* mutants unveils a differential accumulation of transcripts encoding for enzymes involved in carbon partitioning. According to these studies, some enzymes involved in carbon flux decreased (phospho*enol*pyruvate carboxylase, NAD-malic enzyme, glucose-6-P dehydrogenase) or increased (NAD-malate dehydrogenase) their activities compared to the wild-type line. Taken together, our data indicate that a deficiency in the cytosolic GAPC activity results in modifications of carbon flux and mitochondrial dysfunction, leading to an alteration of plant and embryo development with decreased number of seeds, indicating that GAPC-1 is essential for normal fertility in Arabidopsis plants.

Glyceraldehyde-3-P dehydrogenases (GAPDHs) are enzymes conserved in all living organisms, where they play a central role in the carbon economy of the cells. Higher plants possess four distinct isoforms of GAPDHs: (1) GAPC, a cytosolic, phosphorylating, NAD-specific GAPDH catalyzing the conversion of glyceraldehyde-3-P (Ga3P) to 1,3-bisphosphoglycerate; (2) NP-GAPDH, a cytosolic non-phosphorylating NADP-dependent GAPDH that catalyzes the oxidation of Ga3P to 3-phosphoglycerate (3PGA; Valverde et al., 2005); (3) GAPA/B, a phosphorylating, NADP-specific GAPDH involved in photosynthetic $CO_2$ fixation in chloroplasts (Cerff and Chambers, 1979); and (4) GAPCp, involved in glycolytic energy production in non-green plastids (Petersen et al., 2003).

Much is known concerning the gene structure, evolution, and functional properties of GAPDHs in algal systems (Koksharova et al., 1998; Fillinger et al., 2000; Perusse and Schoen, 2004; Valverde et al., 2005), whereas in higher plants, the characterization of GAPDHs was mainly performed on the chloroplastic isoforms that are activated by thioredoxins (Wolosiuk and Buchanan, 1978; Fermani et al., 2007).

In recent years, detailed studies have been carried out on the structure-function relationships (Mateos and Serrano, 1992; Habenicht et al., 1994; Michels et al., 1994; Petersen et al., 2003; Anderson et al., 2004; Hancock et al., 2005) and kinetic properties (Gomez Casati et al., 2000; Bustos and Iglesias, 2002, 2003; Iglesias et al., 2002) of the cytosolic GAPDHs. However, only a few reports have been focused on their in vivo functions (Hajirezaei et al., 2006; Rius et al., 2006; Wang et al., 2007). It has been proposed that the NP-GAPDH isoform plays a central role in a shuttle system mechanism for the transport of the NADPH generated by photosynthesis from the chloroplast to the cytosol and in providing NADPH for gluconeogenesis (Kelly and Gibbs, 1973a; Rumpho et al., 1983; Habenicht, 1997). Recently, we reported that NP-GAPDH could be important in fruit development and energetic metabolism. Interestingly, a mutation in the *NP-GAPDH* gene induced the expression of the cytosolic GAPC-1 isoform (Rius et al., 2006).

[1] This work was supported by CONICET (grant nos. PIP–6241 to D.F.G.-C., and PIP–6357 and CAI+D'06 to A.A.I.), by ANPCyT (grant nos. PICT'06-00614 to D.F.G.-C.; PICTO03–13241 and 05–13129, PICT'03–14733, and PAV'03–137 to A.A.I.; and PICT'03–13278 to P.C.), and by Fundación Antorchas (grant no. 4306–5 to P.C.).

* Corresponding author; e-mail diego.gomezcasati@intech.gov.ar.

The author responsible for distribution of materials integral to the findings presented in this article in accordance with the policy described in the Instructions for Authors is: Diego F. Gomez-Casati (diego.gomezcasati@intech.gov.ar).

[C] Some figures in this article are displayed in color online but in black and white in the print edition.

www.plantphysiol.org/cgi/doi/10.1104/pp.108.128769

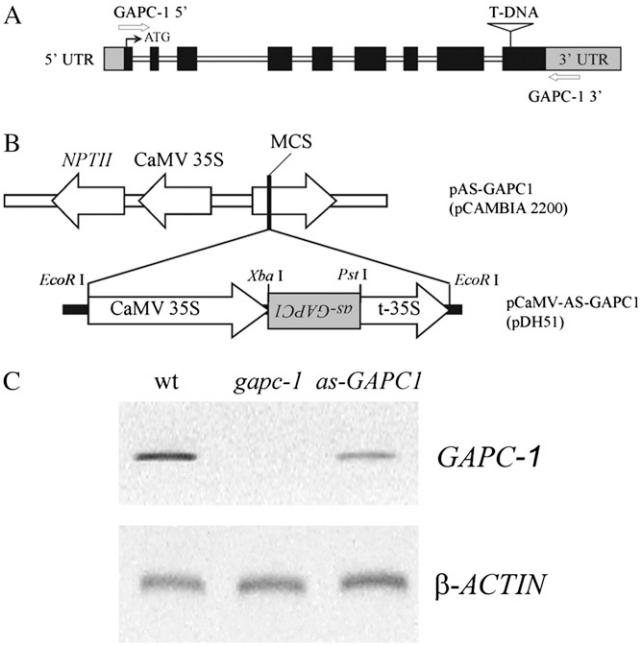


**Figure 1.** Schemes of *gapc-1* null mutant and the antisense construction *as-GAPC1*. A, Intron-exon organization of *GAPC-1* gene of an Arabidopsis T-DNA insertional mutant line (SALK_010839). Arrows show the locations and directions of primers used to screen for *gapc-1* mutant (GAPC-1 5′, GAPC-1 3′). The structure of the T-DNA is not drawn to scale. The *GAPC-1* gene contains nine exons and eight introns. The white triangle shows the T-DNA position in the ninth exon region of *GAPC-1*. B, Schematic representation of the antisense gene (*as-GAPC1*) used to generate transgenic plants expressing a fragment (418 bp) of *GAPC-1* in antisense orientation. The coding sequence of Arabidopsis *GAPC-1* was cloned under the control of cauliflower mosaic virus 35S (CaMV35S) promoter from pDH51 vector and then subcloned on pCAMBIA 2200 multiple cloning site (*Eco*RI site). MCS, Multiple cloning site; t-35S, 35S terminator; *NPTII*, kanamycin resistance gene. C, Steady-state levels of *GAPC-1* mRNA in wild-type, mutant *gapc-1*, and transgenic *as-GAPC1* plants. Total RNA was extracted from 42-d-old leaves and reverse transcribed using random hexamers and then amplified with *GAPC-1*-specific primers. The housekeeping gene *β-ACTIN* (At3g18780) was used as internal control.

The importance of GAPC in photosynthetic tissues has been widely reported; however, only a few reports have described its function in heterotrophic tissues (Fernie et al., 2004; Hajirezaei et al., 2006). Furthermore, GAPC-1 is cytoskeletally associated in many organisms including plants (Chuong et al., 2004). Additionally, it was found associated to other glycolytic enzymes, both in the cytoskeleton and in the mitochondria of Arabidopsis (*Arabidopsis thaliana*; Giege et al., 2003; Holtgrawe et al., 2005). Thus, it was postulated that glycolytic proteins may be important in mitochondrial energetic metabolism and in regulating mitochondrial functions (Giege et al., 2003). Additionally, the coexistence of GAPC and NP-GAPDH in the cytosol establishes a bypass of carbon flux during the glycolysis, which very likely improves the flexibility to respond to environmental stresses. However, the precise consequences of these alternative pathways on the carbon economy and the growth and development of plants have not been explored.

In this work, we isolated and characterized two lines exhibiting a GAPC-1 deficiency: a null mutant line of Arabidopsis deficient in GAPC-1 expression (*gapc-1*, SALK_010839) and a transgenic line expressing the antisense version of the *GAPC-1* gene (At3g04120, *as-GAPC1*). Both lines exhibited defects in fertility, with alterations in seed and fruit development, suggesting that GAPC-1 is essential in these organs. The molecular, biochemical, and physiological studies of these lines indicate that this enzyme plays critical and pleiotropic roles, being essential for the maintenance of cellular ATP levels and carbohydrate metabolism and required for full fertility in Arabidopsis.

## RESULTS

### Identification of a *gapc-1* Mutant and Construction of the Antisense *as-GAPC1* Line

To evaluate the possible function(s) of the *GAPC-1* gene in Arabidopsis, we selected a T-DNA insertion mutant from the Arabidopsis Biological Resource Center (The Ohio State University, Columbus, OH) seed stock (SALK_010839, *gapc-1*). *GAPC-1* (At3g04120;

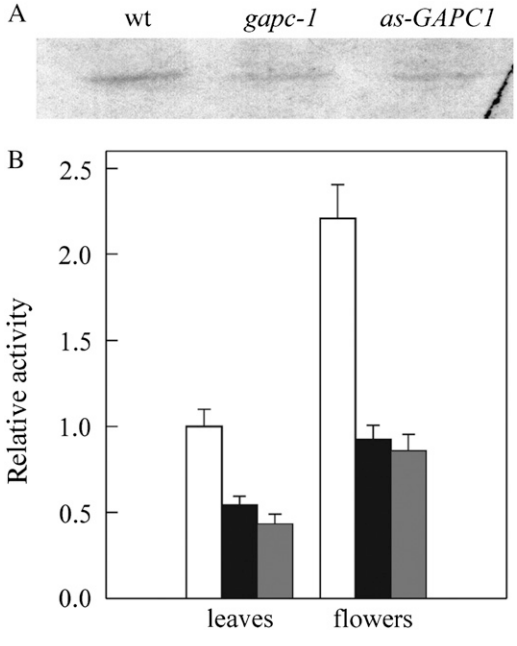


**Figure 2.** Analysis of GAPC by western blot and enzyme activity. A, Western-blot detection of GAPC protein in wild type, *gapc-1* mutants, and transgenic *as-GAPC1* from leaves extracts, using serum anti-GAPC from *Triticum aestivum*. B, NAD-GAPDH activity determined in leaf and flower crude extracts from wild-type (white bars), *gapc-1* (black bars), and *as-GAPC1* (gray bars) plants. The value 1.0 of relative activity represents 22.4 mU mg protein$^{-1}$. Values are the mean ± SD of four independent replicates.

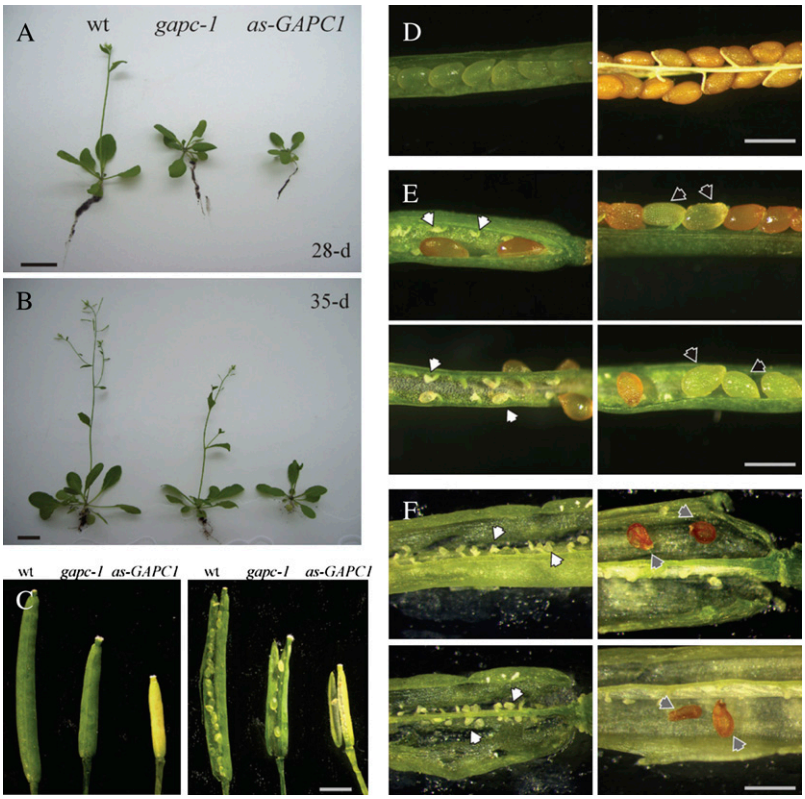


**Figure 3.** Phenotypic analysis of *gapc-1* and *as-GAPC1* plants. A and B, Phenotype comparison of wild-type, *gapc-1*, and *as-GAPC1* plants of Arabidopsis at different stages of development: 28-d-old (A) and 35-d-old (B) growth plants. Bar = 1.0 cm. C, Morphology of siliques from wild-type, *gapc-1*, and *as-GAPC1* plants: closed siliques (right); opened siliques (left). Siliques were from 8 to 9 DPA plants. Bar = 0.2 cm. D to F, Siliques from wild-type (D), *gapc-1* (E), and *as-GAPC1* (F) plants (8–9 DPA); immature siliques (left column) or 12 to 13 DPA mature siliques (right column). White arrows, Aborted seeds; black arrows, empty embryonic sacs; gray arrows, empty seeds. Bar = 0.1 cm. [See online article for color version of this figure.]

1,017 bp) is composed of nine exons and eight introns, and in *gapc-1* plants the T-DNA is inserted in the ninth exon (Fig. 1A). *gapc-1* homozygous plants were isolated using PCR screening, and segregation analysis and DNA gel-blot hybridization indicate that the mutant plants contained only one copy of T-DNA (data not shown).

To obtain a second GAPC-1-deficient line, we constructed a transgenic antisense line (*as-GAPC1*) by transformation with pCAMBIA 2200 plasmid (Hajdukiewiez et al., 1994; Fig. 1B). The expression of *GAPC-1* in null mutants and *as-GAPC1* plants verified by reverse transcription (RT)-PCR analysis shows that *GAPC-1* mRNA is absent in *gapc-1* plants, confirming that the T-DNA insertion impairs GAPC expression (Fig. 1C). In the *as-GAPC1* line, there is a 30% decrease in *GAPC-1* transcripts compared to wild-type plants (Fig. 1C). The GAPC protein levels determined by western blot using specific antibodies show a decrease of 23% ± 5% and 27% ± 8% in *gapc-1* and *as-GAPC1* plants, respectively (Fig. 2A). Moreover, we determined that total GAPC activity is 50% decreased in leaves and flowers of both lines (Fig. 2B). Although we observed a complete absence of the *GAPC-1* transcript in the *gapc-1* line, the amount of protein was reduced in a way that the decrease in GAPC total activity was only about 50% of that determined for wild-type plants. This very likely results from the activity of: (1) other GAPC isoforms encoded by *GAPC-2* (At1g13440), *GAPCp-1* (At1g16300), or *GAPCp-2* (At1g79530) in the Arabidopsis genome; or (2) the GAPA/B isoform, which preferentially uses NADPH but also is active in the presence of NADH (Sparla et al., 2004).

### Phenotypic Characterization of *gapc-1* and *as-GAPC1* Plants

Under normal growth conditions, *gapc-1* and *as-GAPC1* plants exhibited retarded growth at different developmental stages compared to wild-type plants (Fig. 3, A and B). While we did not observe differences in the morphology of roots and leaves, flowers and

**Table I.** *Weight, length, and seed number from wild-type, gapc-1, and as-GAPC1 siliques obtained from 6-week-old plants*

| Variable ($n$ = 20) | Wild Type | *gapc-1* | *as-GAPC1* |
|---|---|---|---|
| Silique length (mm) | 12.4 ± 0.8 | 3.5 ± 0.8 | 2.1 ± 1.0 |
| Silique weight (mg) | 4.62 ± 0.51 | 0.36 ± 0.13 | 0.22 ± 0.12 |
| Seeds/silique | 45 ± 5 | 7 ± 3 | 3 ± 1 |

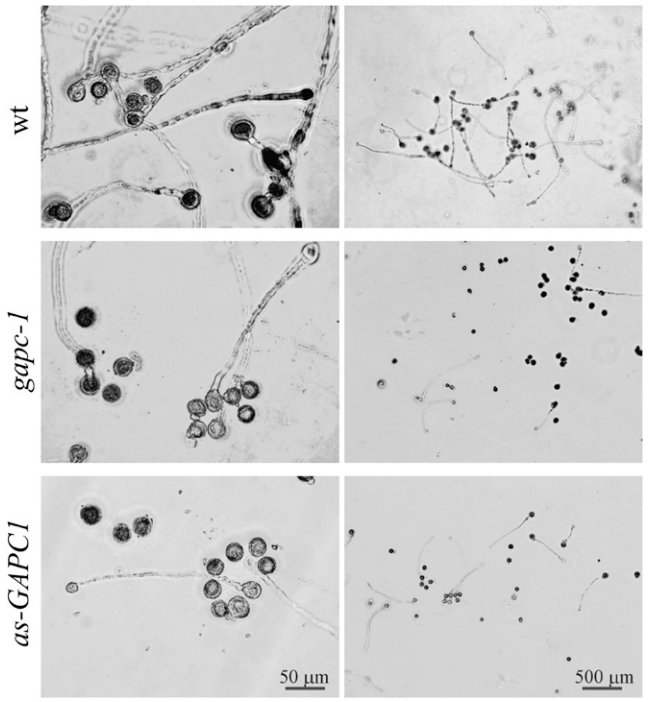


**Figure 4.** In vitro determination of pollen tube formation. Determination of the ability of pollen grains to germinate in vitro. Pollen was obtained from wild-type, *gapc-1*, and *as-GAPC1* plants. Left segment corresponds to 10× detail of right segment for the same pollen line. The scale bar shown on bottom is the same for all the lines.

fruits were severely affected in their morphology, with fruits displaying alterations in their size and weight (Fig. 3C). Wild-type plants have normal amounts of seeds per silique (45 ± 5) and normal morphology (Fig. 3D), whereas *gapc-1* and *as-GAPC1* plants showed aberrant seed development and seed number deficiency (Fig. 3, E and F). The reduced number of seeds (about 12% and 6% for *gapc-1* and *as-GAPC1* plants, respectively) was frequently accompanied by empty embryo sacs (Table I). These results suggest that GAPC activity is essential for zygotic and/or early embryo development. Because GAPC-1-deficient plants have abnormal fruit development, we investigated whether or not pollen viability and/or pollen tube elongation was affected in post-anthesis flowers of these plants. Pollen grains from *gapc-1* and *as-GAPC1* lines showed apparently normal morphology. However, they were not fertile and showed defects in pollen tube germination in vitro. We observed 23% and 21% viable pollen grains in *gapc-1* and *as-GAPC1* lines, respectively, compared to more than 95% of germinated pollen in wild-type plants (Fig. 4).

When the *gapc-1* plants were fertilized with wild-type pollen, the resulting $F_1$ plants exhibited a silique morphology and seed production similar to the wild-type phenotype, with 43 ± 6 seeds per silique and the absence of empty sacs or aborted seeds observed in the mutant line (Fig. 5, A and B). This result suggests that the reduced fertility of the mutant was due to defects in male organs and the female fertility was unaffected.

### Analysis of *gapc-1* Plants

To have a better assessment of the way by which GAPC activity changes determine the observed phenotype, we next compared the transcriptome of *gapc-1* and wild-type plants. Results were analyzed to state a primary relationship between transcript levels and changes in enzyme activities and/or protein function. In addition, we also sought further evidence of changes determining levels of protein and/or activity for many of the implied enzymes.

Microarray analysis revealed alterations in the expression of genes encoding for glycolytic and Krebs cycle enzymes in *gapc-1* plants. As shown in Table II, we observed a down-regulation of several genes involved in these pathways: *GAPC-2*, *NP-GAPDH*, two phosphofructokinase (*PFK*) genes, two pyruvate kinase (*PK*) genes, and a triose-P isomerase (*TPI*) gene.

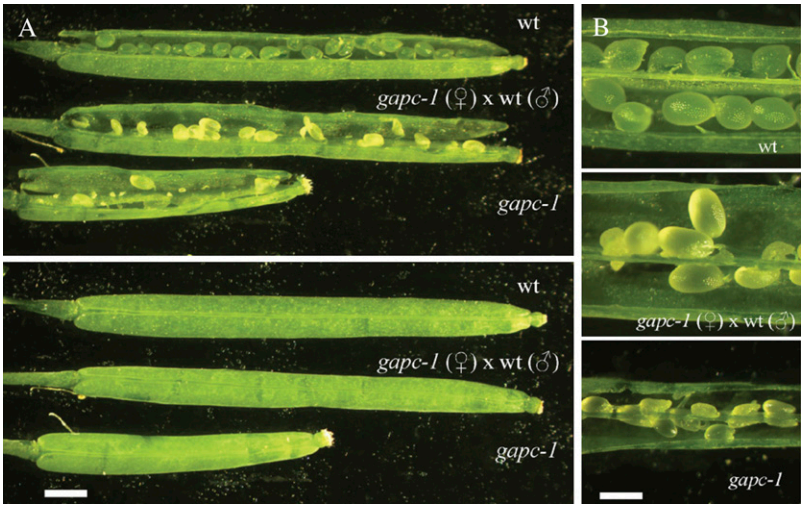


**Figure 5.** Morphology of the siliques from plants after crossing *gapc-1* (♀) × wild type (♂) compared with wild type and homozygous mutant *gapc-1*. Shown are silique size and seed production restoration of homozygous *gapc-1* after pollination with pollen wild type. A, Siliques from wild type (top), *gapc-1* (bottom), and cross *gapc-1* × wild type (middle). Bar = 1 mm. B, Zoom from A. Bar = 0.4 mm. [See online article for color version of this figure.]

**Table II.** *List of selected genes differentially expressed in gapc-1 null mutants in comparison to wild-type plants*

The expression ratio relative to the control is indicated. The full list of expressed genes can be downloaded from Gene Expression Omnibus (accession no. GSE3540).

| Function[a] | At Locus | Relative Fold (Arithmetic) | Localization |
|---|---|---|---|
| NAD-dependent glyceraldehyde-3-P dehydrogenase (GAPC-1) | At3g04120 | 0.05 | Cytosol |
| NAD-dependent glyceraldehyde-3-P dehydrogenase (GAPC-2) | At1g13440 | 0.29 | Cytosol |
| NADP-dependent glyceraldehyde-3-P dehydrogenase (NP-GAPDH) | At2g24270 | 0.06 | Cytosol |
| Phosphofructokinase | At4g26270 | 0.19 | Cytosol |
| | At5g61580 | 0.30 | Cytosol |
| Pyruvate kinase | At3g25960 | 0.32 | Cytosol |
| | At3g52990 | 0.32 | Cytosol |
| Triose-P isomerase | At3g55440 | 0.14 | Cytosol |
| Malate dehydrogenase (NAD-dependent) | At3g53910 | 3.0 | Glycosomal-mitochondria |
| Malate dehydrogenase (NAD-dependent) | At5g56720 | 2.4 | Cytosol |
| Phospho*enol*pyruvate carboxylase | At3g14940 | 0.25 | Unknown |
| | At2g42600 | 0.5 | Unknown |
| Glc-6-P dehydrogenase | At5g13110 | 0.7 | Chloroplast |
| | At1g24280 | 0.6 | Chloroplast |
| NAD-malic enzyme | At2g13560 | 0.7 | Mitochondria |
| Citrate synthase | At3g60100 | 0.4 | Mitochondria |
| Succinate dehydrogenase-Fe-S subunit | At3g27380 | 0.2 | Mitochondria |
| Aconitase | At2g05710 | 0.4 | Mitochondria |
| | At4g26970 | 0.3 | Mitochondria |
| Pyruvate decarboxylase | At5g54960 | 0.22 | Cytosol |
| Rubisco small subunit | At1g67090 | 0.28 | Plastid |
| Rubisco large subunit | At1g14030 | 3.1 | Plastid |
| | At4g20130 | 2.9 | Plastid |
| Rubisco activase | At2g39730 | 0.16 | Plastid |
| Peroxiredoxin thioredoxin-dependent peroxidase 2 (TPX2) | At1g65970 | 5.8 | Mitochondria-peroxisome cytosol |
| Peroxidase (PER62) | At5g39580 | 5.2 | Endomembrane |
| PER41 | At5g05340 | 3.2 | Endomembrane |
| PER52 | At4g17690 | 6.5 | Endomembrane |
| PER9 | At1g44970 | 3.3 | Endomembrane |
| PER2 | At1g05250 | 8.2 | Endomembrane |
| PER31 | At3g28200 | 0.39 | Extracellular |
| Catalase 1 | At1g20630 | 0.71 | Mitochondria-peroxisome |
| Catalase 2 | At4g35090 | 0.5 | Mitochondria-peroxisome |
| Catalase 3 | At1g20620 | 0.37 | Mitochondria-peroxisome |
| Alternative oxidase 2 | At5g64210 | 2.6 | Mitochondria |
| Peroxiredoxin | At3g06050 | 0.95 | Mitochondria |
| Superoxide dismutase [Cu-Zn] | At5g18100 | 4.0 | Peroxisome |
| Superoxide dismutase B [Fe] | At4g25100 | 0.44 | Plastid |
| Superoxide dismutase A [Mn] | At3g10920 | 0.43 | Mitochondria |
| Glutathione *S*-transferase 6 | At2g47730 | 0.42 | Plastid |

[a]Results of BLASTN query of Arabidopsis genome sequence.

Conversely, we observed an up-regulation of two malate dehydrogenase (*NAD-MDH*) genes. As shown in Table II, there is also an alteration in the transcript levels of several genes related to photosynthesis, such as *Rubisco SSU* (At1g67090), *Rubisco LSU* (At1g14030 and At4g20130), and *RCA* (for Rubisco activase; At2g39730). Furthermore, several genes involved in the TCA cycle showed decreased expression: citrate synthase (At3g60100), succinate dehydrogenase (*SDH*; At3g27380), and aconitase (*ACO*; At2g05710 and At4g26970) genes. Also, several genes encoding for enzymes related to stress responses showed altered expression, such as different peroxidase (*PER*) isoforms, a peroxiredoxin (*PEROX*; At1g65970) isoform, an alternative oxidase (*AOX*; At5g64210) isoform, and three isoforms of catalase (*CAT*s). Thus, microarray results suggest that mutants have an altered metabolism, which can induce a stress situation that could

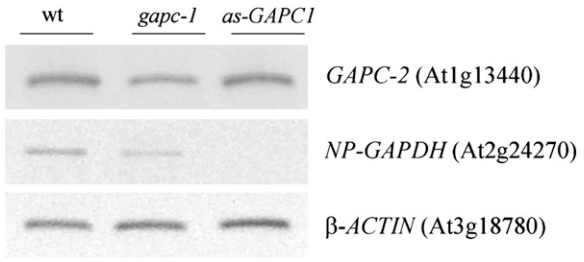


**Figure 6.** Analysis of *GAPC-2* and *NP-GAPDH* transcripts by RT-PCR. Steady-state levels of *GAPC-2* and *NP-GAPDH* transcripts from wild-type, *gapc-1*, and *as-GAPC1* plants. Total RNA was reversed transcribed and then amplified using specific primers. The housekeeping *β-ACTIN* was used as internal control.

account for the delayed growth observed in the GAPC-deficient plants.

As described above, GAPC and NP-GAPDH participate in a bypass step of the glycolysis in plants, catalyzing the production of 3PGA, NADH, and ATP or 3PGA and NADPH, respectively. To further characterize the regulation of this bypass, we analyzed the expression of *NP-GAPDH* in *gapc-1* and *as-GAPC1* plants. A decrease of 25% and 92% in the expression of *NP-GAPDH* in *gapc-1* and *as-GAPC1*, respectively, was observed (Fig. 6), in agreement with the decrease determined by microarray analysis (Table II) and also with the decrease in NP-GAPDH-specific activity (Fig. 7A). This is in contrast to the results obtained with *np-gapdh* mutant plants, where the expression of *GAPC-1* is induced in the absence of *NP-GAPDH*. In addition, we did not observe an up-regulation of genes encoding for Glc-6-P dehydrogenase (G6PDH) isoforms either by microarrays or RT-PCR experiments as was observed in the *np-gapdh* plants (Rius et al., 2006). These data suggest that differences in the regulation or in the compensatory responses of *GAPC-1* and *NP-GAPDH* genes exist in *np-gapdh* and *gapc-1* mutant lines. In addition to GAPC-1, other cytosolic GAPDH isoforms could contribute to the maintenance of the carbon flux through the glycolytic pathway, such as GAPC-2. Therefore, the expression of *GAPC-2* was analyzed. As shown in Figure 6, we found 48% and 37% decreases of *GAPC-2* mRNA levels in *gapc-1* and *as-GAPC1* lines, respectively.

As mentioned above, microarray data from *gapc-1* plants showed an alteration in the level of transcripts encoding for glycolytic and energy metabolism enzymes (Table II). To assess the impact of alterations in gene expression observed in microarrays, we evaluated the activity of several enzymes involved in both pathways (Fig. 7A). A 25% decrease in PK activity was detected in *gapc-1* plants. This correlates with the 74% and 57% decreases in the two *PK* genes expression determined by RT-PCR for *gapc-1* and *as-GAPC1* plants (Fig. 7B) and microarray experiments with *gapc-1* mutants (Table II). We also observed decreases in the activity of other enzymes in the mutant plants: 49% for phospho*enol*pyruvate carboxylase (PEPC), 24% for NAD-malic enzyme (NAD-ME), and 39% for G6PDH (Fig. 7A). The decrease in several glycolytic transcripts such as the two *PK* genes and the inhibition of PK activity (the primary point of regulation of plant glycolysis), as well as the inhibition of other glycolytic enzymes, gives strong support that GAPC-1 deficiency lead to an inhibition of carbohydrate metabolism.

Russell and Sachs (1989) and Yang et al. (1993) have shown that glycolytic genes, whose functions are

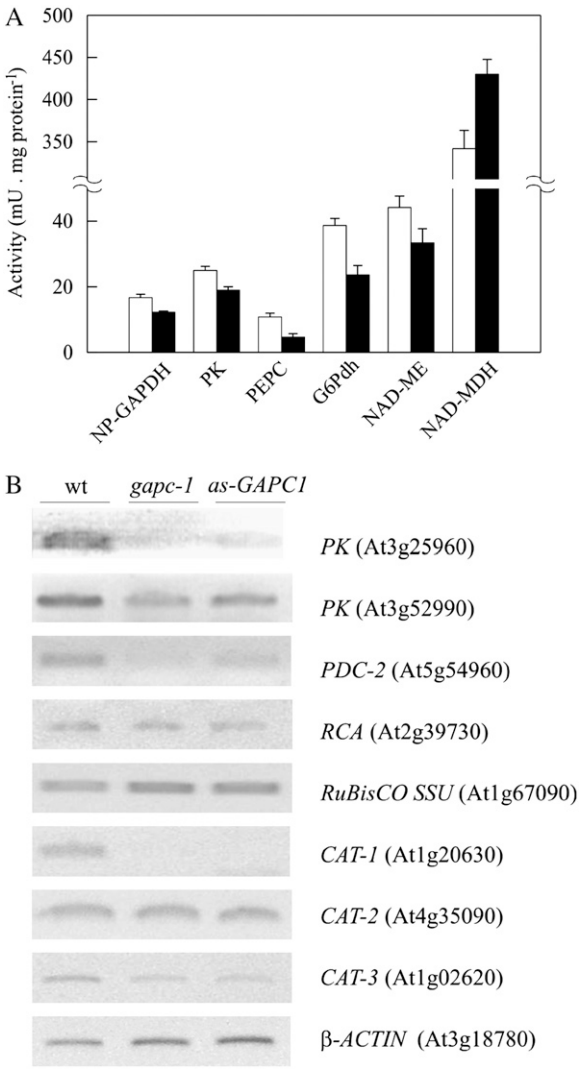


**Figure 7.** Enzyme activity and RT-PCR of oxidative stress and carbon metabolism enzymes. A, Specific activity of enzymes involved in carbohydrate metabolism. NP-GAPDH, PK, PEPC, G6PDH, NAD-ME, and NAD-MDH activity determined in wild-type and *gapc-1* leaf extracts. One unit (U) is defined as quantity of micromoles of NADH or NADPH produced or consumed per minute at the temperature specified in the "Materials and Methods" section for each enzyme. B, RT-PCR analysis of genes involved in oxidative stress and carbon metabolism from wild-type, *gapc-1*, and *as-GAPC1* plants. Total RNA was reversed transcribed and then amplified using specific primers. The housekeeping *β-ACTIN* was used as internal control. SS, Small subunit.

**Table III.** *Determination of metabolite levels in wild-type, gapc-1, and as-GAPC1 plants*

| Compound[a] | Wild Type | *gapc-1* | *as-GAPC1* |
|---|---|---|---|
| Pyruvate | 8.6 ± 1.4 | 2.7 ± 0.6 | 1.9 ± 0.4 |
| Malate | 4.3 ± 0.9 | 7.6 ± 1.2 | 6.8 ± 1.0 |
| Citrate | 9.4 ± 1.5 | 3.7 ± 0.5 | 3.2 ± 0.6 |
| Isocitrate | 1.1 ± 0.2 | 0.6 ± 0.2 | 0.3 ± 0.1 |

[a]Pyruvate levels are expressed in nmol/g fresh weight. Malate, citrate, and isocitrate levels are expressed in μmol/g fresh weight.

required for both glycolysis and fermentation, were expressed at high levels under normoxia, but could be induced further by anoxia or hypoxia. The pyruvate decarboxylase (*PDC*), a gene that functions in alcoholic fermentation, is expressed at extremely low levels in plant cells under normal growth conditions and its expression is strongly induced by hypoxia or anoxia (Conley et al., 1999). A study on the expression of *PDC-2* in leaves from wild-type, *gapc-1*, and *as-GAPC1* plants by RT-PCR shows that *PDC-2* transcript is accumulated at lower levels in GAPC-deficient plants than in wild-type plants (Fig. 7B).

As described above, some genes related to photosynthesis, for example, *Rubisco SSU* and *RCA*, were decreased in microarray analysis. We confirm the decrease in *RCA* transcript levels (about 50%) by RT-PCR analysis. However, a slight increase of *Rubisco SSU* mRNA expression was observed (Fig. 7B). Furthermore, the transcription of many genes encoding for enzymes related to stress responses such as the three catalases was repressed (Fig. 7B; see also Table II). Thus, microarray and RT-PCR results suggest that mutants have an altered photosynthetic and carbon metabolism, which can induce a stress situation that could account for delayed growth.

### *gapc-1* and *as-GAPC1* Plants Show Changes in the Levels of Glycolytic and TCA Intermediates

To evaluate the effect of the GAPC deficiency in glycolytic or TCA intermediates, we quantified the levels of pyruvate, the end product of glycolysis, and malate, the product of the alternative glycolytic pathway. Furthermore, we determined the levels of two metabolites of the TCA cycle, citrate and isocitrate.

The *gapc-1* and *as-GAPC1* plants accumulate 31% and 22%, respectively, of the pyruvate levels compared to the wild type, whereas there is an increase of about 1.7-fold in the accumulation of malate in both lines. Indeed, *gapc-1* and *as-GAPC1* plants showed a reduction in TCA intermediate levels such as citrate (40% and 32%, respectively) and isocitrate (54% and 27%, respectively; Table III).

### *gapc-1* Plants Show Reduced Levels of Oxygen Uptake and ATP, and Reduced Expression and Activity of TCA Cycle Enzymes

It has been demonstrated that GAPC-1 and other glycolytic enzymes are associated with the mitochondrial outer membrane in Arabidopsis (Giege et al., 2003). The respiratory pathways of glycolysis, the TCA cycle, and the mitochondrial electron transport chain are ubiquitous throughout nature. Although the series of enzymes and proteins that participate in these pathways have long been known, their regulation and control are much less well understood (Fernie et al., 2004). GAPC-1 deficiency in mutant plants could be affecting the carbon flux units destined to the TCA cycle. This would affect the respiratory chain function and $O_2$ uptake, with consequences on the ATP produced during oxidative phosphorylation in the mitochondria. To determine the effect of GAPC-1 deficiency on mitochondrial function, we measured the oxygen uptake in mature rosette leaves (6 weeks old) and flowers. Our results show a decrease of 39.5% in leaf respiration in *gapc-1* mutants compared to wild-type plants (Fig. 8A). Furthermore, flowers also showed a decrease of 23% in oxygen uptake compared to the wild type.

The energetic status of the *gapc-1* line was evaluated by measuring total ATP levels. We found 38% and 29.4% decreases in the ATP concentration in mutant

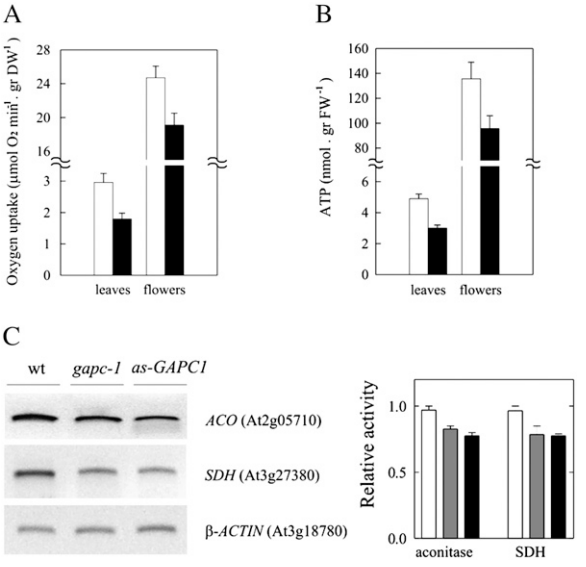


**Figure 8.** Measurement of oxygen uptake, ATP levels, and analysis of the expression and activity of TCA cycle enzymes. A, Determination of $O_2$ evolution (μmol $O_2$ $min^{-1}$ $mg^{-1}$ dry weight) in detached leaves and flowers from wild-type (white bars) and *gapc-1* plants (black bars). B, ATP levels determined in wild-type (white bars) and *gapc-1* (black bars) Arabidopsis rosettes leaves and flowers. C, Left, RT-PCR analysis of *ACO* (At2g05710) and *SDH* (At3g27380) transcripts involved in TCA cycle determined in wild-type, *gapc-1*, and *as-GAPC1* plants. Total RNA was reversed transcribed and then amplified using specific primers. The housekeeping *β-ACTIN* was used as internal control. C, Right, Enzymatic activity of aconitase and SDH in wild-type (with bars), *gapc-1* (gray bars), and *as-GAPC1* plants (black bars). Each enzymatic assay was performed using 10 μg total proteins from isolated mitochondrial fraction. The activity of each enzyme in wild-type plants was used as a reference value.

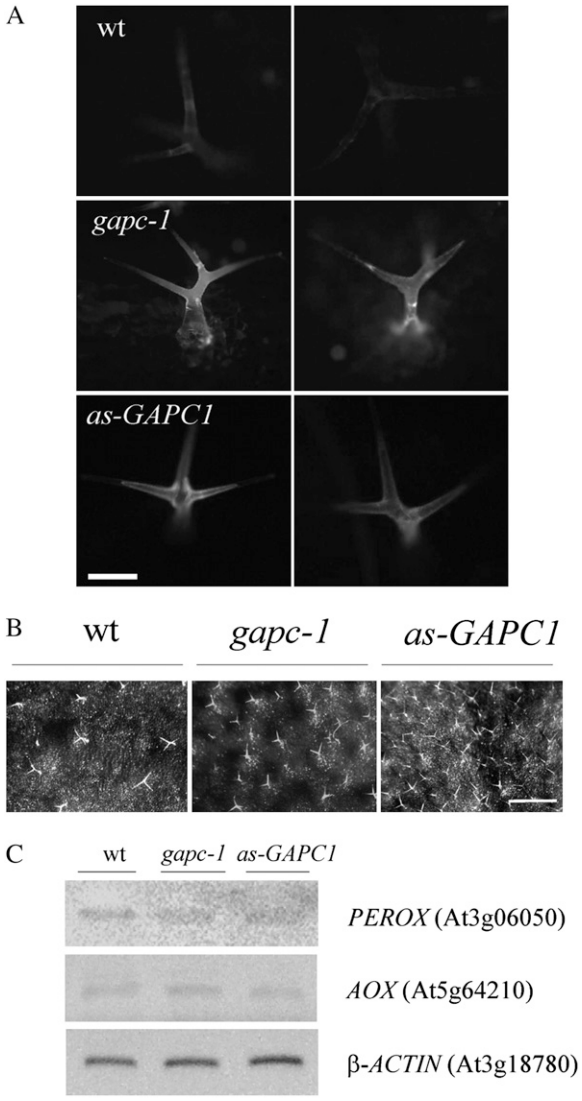


**Figure 9.** Determination of ROS, trichome density, and RT-PCR analysis of genes involved in ROS responses. A, Histochemical detection of ROS by $H_2$DCFA. Fluorescence was visualized by microscopy after incubation of leaves from wild-type, *gapc-1*, and *as-GAPC1* lines with $H_2$DCFDA. Figures show the fluorescence of two representative trichomes from each line. B, Trichome distribution on adult rosettes leaves of wild type, *gapc-1* mutant, and *as-GAPC1* transgenic line. C, RT-PCR analysis of *PEROX* and *AOX* genes involved in ROS metabolism from wild-type, *gapc-1*, and *as-GAPC1* plants. Total RNA was reversed transcribed and then amplified using specific primers. The housekeeping *β-ACTIN* was used as internal control.

leaves and flowers, respectively (Fig. 8B). The results suggest that GAPC-1 deficiency has an important effect on ATP levels, in correlation with the decrease in the respiration rate observed in the mutant plants (Fig. 8A).

The decrease in ATP pools and the reduction of the respiration rate in mutant plants correlate with a reduced expression of genes involved in the TCA cycle such as *ACO* and *SDH* determined by RT-PCR (Fig. 8C). This is in agreement with the observed decrease in aconitase (15% and 20% in *gapc-1* and *as-GAPC1* plants, respectively) and SDH activity (about 20% in both lines; Fig. 8C). Taken together, our results suggest that the GAPC-1 deficiency affects not only the glycolysis but also the function of other respiratory pathways, and that this metabolic deficit could be the cause of the phenotypes observed in reproductive tissues, which depend mainly on respiration to obtain energy.

### *gapc-1* and *as-GAPC1* Plants Exhibit Increased Reactive Oxygen Species Accumulation and Higher Density of Trichomes

Recently, it has been suggested that GAPC plays a regulatory role in reactive oxygen species (ROS) signaling in plants (Hancock et al., 2005). To evaluate the consequences of GAPC-1 deficiency, we determined ROS levels in *gapc-1* and *as-GAPC1* lines by histochemical detection using 2′,7′-dichlorofluorescein diacetate ($H_2$DCFDA). We found an increase in ROS accumulation, as the fluorescence in trichomes is higher in both lines compared to wild-type plants (Fig. 9A). Furthermore, an increase in the trichome density was observed in null mutants and antisense lines (Fig. 9B). A special role in detoxification has been assigned to trichomes of *Brassica juncea* that accumulate cadmium (Salt et al., 1995). Also, it has been proposed that Arabidopsis trichome cells have a role in GSH biosynthesis, and they may also function as a sink during detoxification processes, suggesting that trichomes may have a role in xenobiotic conjugation (Gutierrez-Alcala et al., 2000).

Microarray data also show that transcript levels for several genes encoding proteins that participate in oxidative stress response, such as peroxidases (*PER62*, *PER41*, *PER52*, *PER9*, and *PER2*) and superoxide dismutase [Cu-Zn], show increased levels in *gapc-1* plants. In addition, we measured by RT-PCR the mRNA levels of other genes encoding for proteins involved in stress responses, such as *PEROX* and *AOX* (Sweetlove et al., 2002), which showed a slight change in expression (Fig. 9C). All together, these data support the existence of increased oxidative stress in GAPC-1-deficient plants.

## DISCUSSION

To investigate other possible physiological functions of GAPC-1, we characterized two GAPC-deficient lines: a T-DNA insertional mutant (SALK_010839, *gapc-1*) and an antisense line, *as-GAPC1*. We found evidence that GAPC-1 plays an important role and is required for full fertility in Arabidopsis plants. The knockout mutant *gapc-1* is null in terms of *GAPC-1* expression, and the *as-GAPC1* line displayed a decrease in the expression of *GAPC-1* transcript. Accordingly, both lines showed lower levels of GAPC protein by western-blot analysis

**Table IV.** *List of primers used in RT-PCR and mutant analysis*

| Gene (At Locus) | Primers, Forward/Reverse |
|---|---|
| *GAPC-1* (At3g04120) | TCTCATATGCTGACAAGAAGAT |
| | CACTCCCTATCATTCGAGATCTGCTTC |
| *GAPC-2* (At1g13440) | GAGTACATGACCTACATG |
| | TCAACCACACACAAACTCGAGCCGGTG |
| *NP-GAPDH* (At2g24270) | AGACATATGGCCGGGACTGGATTGTTT |
| | ACCCTCGAGCTAACCCATAGAGTAAGAAGGT |
| *RBCS-1* (At1g67090) | AAAGGTACCATGGCTTCCTCTATGCTC |
| | AAACATATGAAGGTCAGGAGGTAAGA |
| *CAT1* (At1g20630) | GATAAGCTACTCCAGACCCGGA |
| | CTGAGACCAGTAAGAGATCCA |
| *CAT2* (At4g35090) | GATAAGCTGCTTCAAACCCGTG |
| | CTGAGACCAGTAAGAGATCCA |
| *CAT3* (At1g20620) | ACGACAAGCTGCTCCAGTGTA |
| | CTGAGACCAGTAAGAGATCCA |
| *PK* (At3g25960) | ATGCATTCCAGTCATCTCC |
| | TGGTGTCTCCTTTCTTCAC |
| *PK* (At3g25960) | ATGGAGATGTTACTTGGTG |
| | TCCTTGTATCTTGTAATCAAT |
| *RCA* (At2g39730) | ATGGCCGCCGCAGTTTCCAC |
| | TAGGAGCTTGGAAGACAGAG |
| *PDC-2* (At5g54960) | AGATCGGATCTATCGACGCG |
| | GGTTTGGTTCGGCGATTAGG |
| *AOX* (At5g64210) | ATTTTTTCAGAGACGATA |
| | GCGAATGTCAGAAGCAAA |
| *PEROX* (At3g06050) | ATCTTCAAGGGGAAGAAA |
| | GCCGACCATCTCTCAGAC |
| *SDH* (At3g27380) | AAACATATGGCGGAGGCGGAAACAAAA |
| | AAACTCGAGACGCTGAAGTTGCTTGAT |

(Figs. 1 and 2) and reduced activity in leaves and flowers (Fig. 2B). Western-blot analysis performed in *gapc-1* and *as-GAPC1* plants revealed the presence of a protein band that reacts with a-GAPC antibodies. This can be due to the expression of GAPC-2, a cytosolic isoform of GAPC having high structural similarity with GAPC-1, whereas GAPC-2, GAPCp, and/or GAPA/B isoforms could contribute to the NADH-dependent residual activity observed in the two lines.

Both *gapc-1* and *as-GAPC1* plants exhibited a delay in growth. Indeed, both lines presented an alteration in silique morphology and seed production. The defect in pollen tube germination and the restoration of viable seed production after crossing experiments using wild-type pollen indicate that GAPC-1 function is important in male organs and suggest that the decrease in GAPC-1 activity impairs the mitochondrial function required for normal pollen production (Heiser et al., 1997). The phenotypes obtained showed that GAPC activity is essential in reproductive tissues and revealed the importance of the *GAPC-1* gene in plant development and fructification. To link this phenotype with the underlying mechanisms determining it, we investigated the effects of the mutation on the *GAPC-1* gene in glycolysis by transcriptome analysis of *gapc-1* plants. Our results demonstrate that this line exhibited a down-regulation of several genes involved in glycolysis: *NP-GAPDH*, *GAPC-2*, *TPI*, *PFK*s, and *PK*. Furthermore, we confirmed that the glycolytic pathway is altered in the GAPC-deficient plants by measuring the activity of some of the enzymes of this pathway. It has been reported that PK is the primary point of regulation of glycolysis (Plaxton, 1996; Plaxton and Podestá, 2006). Our results indicate that there is a down-regulation of two genes encoding for cytosolic PKs and also a decrease in PK activity, strongly suggesting a reduction in the glycolytic flux after GAPC-1 reaction. These results are in agreement with previous works (Siddiquee et al., 2004; Rius et al., 2006) that illustrate that blocking the glycolytic pathway at the level of PK or NP-GADPH leads to a down-regulation of several glycolytic genes.

In a previous work, Hajirezaei et al. (2006) demonstrated that the inhibition of phosphorylating GAPC in potato (*Solanum tuberosum*) plants does not greatly affect sugar metabolism in leaves or tubers; however, there was an alteration in the levels of several glycolytic intermediates. It has been suggested that the lack of phosphorylating GAPC can be compensated by other isoforms, such as NP-GAPDH. To investigate this hypothesis, we analyzed the expression of *NP-GAPDH* and *GAPC-2* in *gapc-1* and *as-GAPC1* plants. Interestingly, the mutation in the *GAPC-1* gene did not induce the expression of other cytosolic GAPC isoforms. In contrast to what we observed previously in *np-gapdh* plants (Rius et al., 2006), the mutation on *GAPC-1* produced a decrease in *NP-GAPDH* and *GAPC-2* mRNA levels in both *gapc-1* and *as-GAPC1* lines.

In plants, the glycolytic carbon flux can pass through the GAPC enzyme producing 3PGA, NADH, and ATP or through a metabolic bypass catalyzed by NP-GAPDH producing 3PGA and NADPH, but not ATP. This alternative pathway has energetic and metabolic consequences; it has been proposed to participate in a shuttle of triose-P/phosphate that indirectly transfers photosynthetically reduced $NADP^+$ from chloroplast to cytoplasm during photosynthesis (Kelly and Gibbs, 1973b), but its regulation is not yet completely understood. A recent study has shown that the non-phosphorylating *NP-GAPDH* is up-regulated during inorganic phosphate (Pi) starvation in Arabidopsis, while other genes, including *GAPC-1*, are down-regulated (Wu et al., 2003). It is interesting to note that GAPC-2 has been suggested to play an important role in responses to low-Pi stress, possibly through the regulation of a glycolysis-associated "Pi-pool" and accumulation of anthocyanin pigments in Arabidopsis (Wang et al., 2007). Our previous work demonstrates the up-regulation of *GAPC-1* in *np-gapdh* null mutant plants (Rius et al., 2006). Thus, it is possible that a coordinated regulation of the expression of both genes exists, although not reciprocally, *GAPC-1* to *NP-GAPDH*. However, the specific regulation of this bypass is far from complete.

The deficiency of GAPC-1 activity shows a direct effect on the production of energy, as we measured a decrease in ATP cellular levels in flowers and leaves of the *gapc-1* plants. Indeed, the decrease of pyruvate levels and TCA cycle intermediates suggests a decrease in the carbon flux through the glycolytic pathway to the mitochondria. Pollen development in the anther and the growth of the pollen tube are highly energy-demanding processes. It has been reported that pollen granules contain 20 times more mitochondria per cell than normal vegetative tissues in maize (Gass et al., 2005). Thus, an intense mitochondrial activity occurs during sporogenesis. As described by Giege et al. (2003), GAPC-1 as well as other glycolytic enzymes are physically associated with the external mitochondrial membrane in Arabidopsis. Indeed, the existence of substrate channeling restricts the use of intermediates by competing metabolic pathways and enhances the direct entrance of carbon to respiration, resulting in an increase of ATP production (Graham et al., 2007). In this work, the consequence of GAPC deficiency in *gapc-1* mutants has an important influence on the respiration rate and in ATP, pyruvate, malate, and other TCA cycle metabolite levels, which suggests that the alteration in glycolysis can affect the carbon flux and oxidative phosphorylation in the mitochondria. It is important to note that oxidative phosphorylation is more efficient than glycolysis for ATP production, and the mitochondria is the major supplier of the ATP used in the cytosol (Igamberdiev et al., 1998).

Two major sites of ROS production in plant cells have been reported, one in the chloroplast, where ROS is produced in the photosynthetic electron transport chain, and the other in the mitochondria (Millar et al., 2001; Moller, 2001; Moller and Kristensen, 2004). The null mutants and the *as-GAPC1* lines showed increased ROS accumulation and trichome density and induction of genes involved in stress responses, supporting the existence of increased oxidative stress in both lines. Thus, the increased trichome density observed could be a response to higher levels of ROS. In Arabidopsis, an increment in trichome number after stress treatments or exposure to ionizing radiations was described to be mediated by ROS (Nagata et al., 1999). Indeed, our results are in agreement with the proposed role of GAPC in the control of hydrogen peroxide production (Baek et al., 2008) and in the regulation of ROS signaling in plants (Hancock et al., 2005).

In conclusion, in this work, we studied the effect of the disruption of the *GAPC-1* gene in Arabidopsis plants using *gapc-1* null mutants and antisense lines deficient in GAPC-1 expression. Both lines showed defects in fertility, with alterations of seed and fruit development, suggesting that GAPC-1 and the presence of a full glycolytic pathway are essential in these organs and have an important role in fertility in Arabidopsis. Analysis by microarrays, RT-PCR, and enzymatic activity suggest that a deficiency in GAPC-1 results in an inhibition of glycolysis, mitochondrial dysfunction, and increase of oxidative stress.

## MATERIALS AND METHODS

### Plant Material and Growth Conditions

Arabidopsis (*Arabidopsis thaliana*) var Columbia was used as the wild type. The *gapc-1* mutant plant contains a T-DNA insertion in the ninth exon of the *GAPC-1* gene At3g04120 (SALK_010839; Fig. 1A). The *gapc-1* mutant seeds were obtained from the T-DNA Express Collection at the Salk Institute (http://signal.salk.edu/cgi-bin/tdnaexpress). Seeds were germinated directly in soil and kept at 4°C for at least 72 h before light treatment. Plants were grown in greenhouse conditions at 25°C under fluorescent lamps (Grolux, Sylvania and Cool White, Philips) with an intensity of 150 $\mu$mol $m^{-2}$ $s^{-1}$ using a 16-h-light/8-h-dark photoperiod.

### Identification of Insertional *gapc-1* Mutants

The position of the T-DNA insert was determined by PCR using the following primers: LBb1 (GCGTGGACCGCTTGCTGCAACT; http://signal.salk.edu) and *GAPC-1* (Table IV). Genomic DNA was extracted from leaves using the cetyl-trimethyl-ammonium bromide method described by Sambrook et al. (1989). The genotype was determined by PCR on genomic DNA using primers flanking the insertion point for wild-type plants (*GAPC-1* forward and reverse; Table IV), and LBb1 and *GAPC-1* forward primer pair for the *gapc-1* mutant.

### Isolation of RNA and RT-PCR Analysis

Total RNA from 6-week-old fully expanded rosette leaves collected from pools of six plants was extracted using TRI Reagent (Sigma-Aldrich). First, cDNA synthesis was obtained using total RNA (3 $\mu$g) in the presence of random hexamers and moloney murine leukemia virus RT (USB) according to the manufacturers' instructions. An aliquot (1 $\mu$L) from the RT reaction was used as template in PCR reactions with the corresponding oligonucleotides (Table IV). Semiquantitative RT-PCR analysis was performed on the amplification of products after 16, 20, 24, and 28 PCR cycles using (at least) three

independent samples. Appropriate number of cycles was determined for each cDNA to obtain data during the exponential phase of the PCR reaction. *β-ACTIN* was used as internal control. Specific primer pairs were designed based on the cDNA sequence reported in GenBank for the desired genes. PCR products were analyzed on agarose gels and visualized using ethidium bromide staining and/or transferred onto Hybond N+ membranes (Amersham Biosciences). Probe labeling and membrane hybridization were performed according to the ECL Direct Nucleic Acid Labeling and Detection System protocol (Amersham Biosciences).

## Microarray Experiments and Data Analysis

Arabidopsis oligonucleotide microarrays were fabricated by the University of Arizona and contain 26,000 oligonucleotides (http://www.ag.arizona.edu/microarray/). All analyses were completed as described previously (Rius et al., 2006). Briefly, RNA was isolated from 6-week-old rosette leaves obtained from pools of eight plants, both mutant and wild-type plants, grown as described above. The experimental (mutant) and reference (wild-type) RNA samples were reverse-transcribed and directly labeled with either Cy5-dUTP or Cy3-dUTP fluorescent dye (Amersham Pharmacia Biotech) using random hexamer primers (Invitrogen). After that, labeled samples were mixed and hybridized to the microarrays. The slides were scanned with a GenePix 4000B Scanner (Axon Instruments). Results were obtained by triplicates and using samples from different experiments as biological replicates. Data from multiple experiments were normalized (Bolstad et al., 2003), and signals from spots from different experiments were statistically analyzed using Significance Analysis of Microarrays employing the one-class response (http://www-stat.stanford.edu/~tibs/SAM/; Tusher et al., 2001) cut at a false discovery rate <10%. The microarray data are accessible through http://www.ncbi.nlm.nih.gov/geo/ with accession number GSE3540.

## Bioinformatic Methods

The relative levels of mRNA transcripts for the different genes were determined by densitometric analysis using the Gel Pro Analyzer program (Media Cybernetics).

## Respiration Measurements

Oxygen consumption was measured at 25°C using an air-tight chamber fitted with a Clark type electrode (Hansatech Leaf Disc Electrode unit). Calibration was achieved by a simple 2-point calibration between air (21% $O_2$) and the injection or removal of a known volume of air from the chamber. Zero oxygen was achieved by equilibration with $N_2$ to displace all the $O_2$ present in the chamber. Plants were kept in the dark for 15 min before measurement. Detached Arabidopsis leaves and bud flowers (200–300 mg) were placed in the oxygen electrode chamber. Oxygen concentration was monitored for 15 min.

## Immunoblotting

Leaf extracts obtained from pools of six plants were electrophoresed on 12% SDS-polyacrylamide gels and electroblotted onto a nitrocellulose membrane. Immunoblotting was revealed using affinity-purified antibodies raised against recombinant GAPC of *Triticum aestivum*, and antigenic polypeptides were detected using an alkaline-phosphatase-conjugated secondary antibody (dilution 1:10,000), as described previously (Plaxton, 1989; Bollag et al., 1996). The western-blot experiments were performed by triplicate and the average values ± SD are reported.

## In Vitro Pollen Germination

In vitro pollen germination was determined by incubating released pollen with medium containing 17% (w/v) Suc, 2 mM $CaCl_2$, 1.65 mM $H_3BO_3$, 0.6% (w/v) agar, and 5 mM MES, pH 5.8, as described previously (Busi et al., 2006a). Only freshly anther-dehisced flowers were used for in vitro pollen germination experiments, because pollen grains at this developmental stage show the highest germination percentage. For each experiment, flowers were randomly collected from different plants. Total and germinated pollen grains were counted under a microscope after 6 h of incubation at 25°C with 100% relative humidity (Schnurr et al., 2006).

## Measurement of ATP Pool

Six-week-old rosette leaves and bud flowers from wild-type and *gapc-1* plants frozen with liquid nitrogen were ground to a powder using a chilled mortar and pestle. The powder (20 mg) was homogenized with 60 μL of 0.1 M HCl in a 1.5-mL microtube. The homogenate was centrifuged at 20,000*g* for 10 min at 4°C. The supernatant was filtered through a micro-concentrator Microcon YM-3 (Amicon) at 14,000*g* at 4°C. After neutralization with 1 M Tris-HCl, pH 7.4, the filtrates were used for the measurement of ATP levels. Total cellular ATP content was determined with an ATP bioluminescent assay kit (Sigma-Aldrich) and an LD-400 Luminescence detector (Beckman-Coulter; Wulff and Döppen, 1985). ATP levels are expressed in nmol/g fresh weight. All data were subjected to regression analysis or the Student's *t* test. The standard curve of ATP concentration was prepared from a known amount. Means ± SD ($n = 4$) are significantly different at the $P < 0.05$ probability level.

## Determination of Metabolite Levels

Metabolite levels were assayed spectrophotometrically as described previously (Chen et al., 2002) with minor modifications. Leaves (approximately 300–500 mg) were harvested at the end of the light period, immediately placed in liquid nitrogen, and ground to a powder. Two milliliters of ice-cold 4% (v/v) $HClO_4$ was added to the powder. The suspension was kept on ice for approximately 30 min and then centrifuged 15 min at 20,000*g*. The mixture was neutralized with 5 M $K_2CO_3$ and treated with activated charcoal (washed with HCl). The supernatant was used for the measurement of metabolites (Chen et al., 2002). Reported values are the means of at least four independent measurements ± SE.

## Histochemical Detection of ROS in Arabidopsis Leaves by Fluorometric Assay

The histochemical detection of ROS was performed according to Hempel et al. (1999). Briefly, freshly cut, 6-week-old Arabidopsis rosette leaves were incubated with a solution containing phosphate buffer saline 1× and 5 μM $H_2$DCFDA. The tissues were incubated for 2 min at room temperature in the dark, and then washed for 3 min twice in 1× phosphate buffer saline. Fluorescence was immediately visualized using a Nikon fluorescence microscope (Eclipse E800).

## Enzyme Assays

Homogenates used to determine enzyme activity were prepared as described (Eastmond et al., 2000). Cell-free preparations were obtained from 6-week-old rosette leaves. Leaves (200 mg) were washed, frozen under liquid nitrogen, and ground to a powder. The powdered material was homogenized with 600 μL of buffer containing 50 mM Tris-HCl, pH 8.0, 5 mM EDTA, 1 mM phenylmethylsulfonyl fluoride, and 40 mM 2-mercaptoethanol. The homogenate was centrifuged at 12,000*g* for 20 min at 4°C, and the supernatant was collected. NP-GAPDH, PK, PEPC, G6PDH, NAD-ME, and NAD-MDH were assayed spectrophotometrically at 340 nm at 30°C as described previously (Gomez Casati et al., 2000; Rius et al., 2006). GAPC activity was measured by following the reduction of $NAD^+$. The medium contained 50 mM triethanolamine-HCl, pH 8.5, 4 mM $NAD^+$, 10 mM $Na_3AsO_4$, 1.2 μmol D-Ga3P, and 3 mM dithiothreitol. Reactions were initiated by the addition of Ga3P, and the rate of increase in absorbance was linear for at least 3 to 5 min. Activity increased linearly with increasing enzyme concentration. One unit (U) is defined as the amount of enzyme that catalyzes the formation or consumption of 1 μmol $min^{-1}$ NADPH or NADH under each specified assay condition. SDH activity was measured in mitochondrial fraction with the 2,6-dichlorophenolindophenol method as described previously (Busi et al., 2006b), and aconitase activity was monitored by measuring the formation of cis-aconitate at 240 nm (Li et al., 1999). All the determinations were performed at least by triplicate and the average values ± SD are reported.

## Protein Measurements

Protein concentration was determined by the modified Bradford assay (Bollag et al., 1996) using bovine serum albumin as a standard.

### Cloning of the *GAPC-1* Gene and Production of Transgenic Plants

General molecular techniques such as plasmid DNA isolation, restriction digestion, modification and ligation of DNA, PCR, agarose gel electrophoresis, northern blots, transformation, and culture of *Escherichia coli* were carried out according to standards protocols (Sambrook et al., 1989). To prepare the antisense construct of *GAPC-1*, a *Pst*I/*Xho*I fragment (418 bp) containing the Arabidopsis *GAPC-1* coding sequence was isolated, purified, and cloned downstream from the cauliflower mosaic virus 35S promoter into pDH51 vector (Pietrzak et al., 1986) previously digested with *Sal*I and *Pst*I. After verifying the correct orientation of the insert, the resulting 35S:*as-GAPC* expression cassette was excised as *Eco*RI restriction fragments and subcloned into pCAMBIA 2200 (Hajdukiewiez et al., 1994). The recombinant plasmids were introduced into *Agrobacterium tumefaciens* GV3101 strain by the freeze-thaw method (Weigel and Glazebrook, 2006). Arabidopsis was transformed using the floral dip method (Clough and Bent, 1998). Transgenic plants were selected on Murashige and Skoog solid media containing 40 mg $L^{-1}$ of kanamycin and transferred to soil. The expression of the antisense version of *GAPC*-1 gene was verified by RT-PCR.

## ACKNOWLEDGMENTS

We are grateful to Jose Luis Burgos (Comision de Investigaciones Científicas) for excellent technical assistance and the Arabidopsis Biological Resource Center and the stock donor(s). We thank Drs. María Victoria Busi, Guillermo Santa María, and Alejandro Araya for helpful discussions and critical reading of the manuscript and Dr. Carlos Bartoli for helping with the respiration measurements.

Received August 30, 2008; accepted September 22, 2008; published September 26, 2008.

## LITERATURE CITED

**Anderson LE, Ringenberg MR, Carol AA** (2004) Cytosolic glyceraldehyde-3-P dehydrogenase and the B subunit of the chloroplast enzyme are present in the pea leaf nucleus. Protoplasma **223:** 33–43

**Baek D, Jin Y, Jeong JC, Lee HJ, Moon H, Lee J, Shin D, Kang CH, Kim DH, Nam J, et al** (2008) Suppression of reactive oxygen species by glyceraldehyde-3-phosphate dehydrogenase. Phytochemistry **69:** 333–338

**Bollag DM, Rozycki MD, Edelstein SJ** (1996) Protein Methods, Ed 2. Wiley-Liss, New York

**Bolstad DM, Irizarry RA, Astrand M, Speed TP** (2003) A comparison of normalization methods for high density oligonucleotide array data based on bias and variance. Bioinformatics **19:** 185–193

**Busi MV, Gomez-Casati DF, Perales M, Araya A, Zabaleta E** (2006a) Nuclear-encoded mitochondrial complex I gene expression is restored to normal levels by inhibition of unedited ATP9 transgene expression in Arabidopsis thaliana. Plant Physiol Biochem **44:** 1–6

**Busi MV, Maliandi MV, Valdez H, Clemente M, Zabaleta EJ, Araya A, Gomez-Casati DF** (2006b) Deficiency of Arabidopsis thaliana frataxin alters activity of mitochondrial Fe-S proteins and induces oxidative stress. Plant J **48:** 873–882

**Bustos DM, Iglesias AA** (2002) Non-phosphorylating glyceraldehyde-3-phosphate dehydrogenase is post-translationally phosphorylated in heterotrophic cells of wheat (Triticum aestivum). FEBS Lett **530:** 169–173

**Bustos DM, Iglesias AA** (2003) Phosphorylated non-phosphorylating glyceraldehyde-3-phosphate dehydrogenase from heterotrophic cells of wheat interacts with 14-3-3 proteins. Plant Physiol **133:** 2081–2088

**Cerff R, Chambers SE** (1979) Subunit structure of higher plant glyceraldehyde-3-phosphate dehydrogenases (EC 1.2.1.12 and EC 1.2.1.13). J Biol Chem **254:** 6094–6098

**Chen LS, Lin Q, Nose A** (2002) A comparative study on diurnal changes in metabolite levels in the leaves of three crassulacean acid metabolism (CAM) species, Ananas comosus, Kalanchoe daigremontiana and K. pinnata. J Exp Bot **53:** 341–350

**Chuong SD, Good AG, Taylor GJ, Freeman MC, Moorhead GB, Muench DG** (2004) Large-scale identification of tubulin-binding proteins provides insight on subcellular trafficking, metabolic channeling, and signaling in plant cells. Mol Cell Proteomics **3:** 970–983

**Clough SJ, Bent AF** (1998) Floral dip: a simplified method for Agrobacterium-mediated transformation of Arabidopsis thaliana. Plant J **16:** 735–743

**Conley TR, Peng HP, Shih MC** (1999) Mutations affecting induction of glycolytic and fermentative genes during germination and environmental stresses in Arabidopsis. Plant Physiol **119:** 599–608

**Eastmond PJ, Germain V, Lange PR, Bryce JH, Smith SM, Graham IA** (2000) Postgerminative growth and lipid catabolism in oilseeds lacking the glyoxylate cycle. Proc Natl Acad Sci USA **97:** 5669–5674

**Fermani S, Sparla F, Falini G, Martelli PL, Casadio R, Pupillo P, Ripamonti A, Trost P** (2007) Molecular mechanism of thioredoxin regulation in photosynthetic A2B2-glyceraldehyde-3-phosphate dehydrogenase. Proc Natl Acad Sci USA **104:** 11109–11114

**Fernie AR, Carrari F, Sweetlove LJ** (2004) Respiratory metabolism: glycolysis, the TCA cycle and mitochondrial electron transport. Curr Opin Plant Biol **7:** 254–261

**Fillinger S, Boschi-Muller S, Azza S, Dervyn E, Branlant G, Aymerich S** (2000) Two glyceraldehyde-3-phosphate dehydrogenases with opposite physiological roles in a nonphotosynthetic bacterium. J Biol Chem **275:** 14031–14037

**Gass N, Glagotskaia T, Mellema S, Stuurman J, Barone M, Mandel T, Roessner-Tunali U, Kuhlemeier C** (2005) Pyruvate decarboxylase provides growing pollen tubes with a competitive advantage in petunia. Plant Cell **17:** 2355–2368

**Giege P, Heazlewood JL, Roessner-Tunali U, Millar AH, Fernie AR, Leaver CJ, Sweetlove LJ** (2003) Enzymes of glycolysis are functionally associated with the mitochondrion in *Arabidopsis* cells. Plant Cell **15:** 2140–2151

**Gomez Casati DF, Sesma JI, Iglesias AA** (2000) Structural and kinetic characterization of NADP-dependent, non-phosphorylating glyceraldehyde-3-phosphate dehydrogenase from celery leaves. Plant Sci **154:** 107–115

**Graham JW, Williams TC, Morgan M, Fernie AR, Ratcliffe RG, Sweetlove LJ** (2007) Glycolytic enzymes associate dynamically with mitochondria in response to respiratory demand and support substrate channeling. Plant Cell **19:** 3723–3738

**Gutierrez-Alcala G, Gotor C, Meyer AJ, Fricker M, Vega JM, Romero LC** (2000) Glutathione biosynthesis in Arabidopsis trichome cells. Proc Natl Acad Sci USA **97:** 11108–11113

**Habenicht A** (1997) The non-phosphorylating glyceraldehyde-3-phosphate dehydrogenase: biochemistry, structure, occurrence and evolution. Biol Chem **378:** 1413–1419

**Habenicht A, Hellman U, Cerff R** (1994) Non-phosphorylating GAPDH of higher plants is a member of the aldehyde dehydrogenase superfamily with no sequence homology to phosphorylating GAPDH. J Mol Biol **237:** 165–171

**Hajdukiewiez P, Svab Z, Maliga P** (1994) The small, versatile pPZP family of Agrobacterium binary vectors for plant transformation. Plant Mol Biol **25:** 989–994

**Hajirezaei MR, Biemelt S, Peisker M, Lytovchenko A, Fernie AR, Sonnewald U** (2006) The influence of cytosolic phosphorylating glyceraldehyde 3-phosphate dehydrogenase (GAPC) on potato tuber metabolism. J Exp Bot **57:** 2363–2377

**Hancock JT, Henson D, Nyirenda M, Desikan R, Harrison J, Lewis M, Hughes J, Neill SJ** (2005) Proteomic identification of glyceraldehyde 3-phosphate dehydrogenase as an inhibitory target of hydrogen peroxide in Arabidopsis. Plant Physiol Biochem **43:** 828–835

**Heiser V, Rasmusson A, Thieck O, Brennicke A, Grohmann L** (1997) Antisense repression of the mitochondrial NADH-binding subunit of complex I in transgenic potato plants induces male sterility. Plant Sci **127:** 61–69

**Hempel SL, Buettner GR, O'Malley YQ, Wessels DA, Flaherty DM** (1999) Dihydrofluorescein diacetate is superior for detecting intracellular oxidants: comparison with 2′,7′-dichlorodihydrofluorescein diacetate, 5(and 6)-carboxy-2′,7′-dichlorodihydrofluorescein diacetate, and dihydrorhodamine 123. Free Radic Biol Med **27:** 146–159

**Holtgrawe D, Scholz A, Altmann B, Scheibe R** (2005) Cytoskeleton-associated, carbohydrate-metabolizing enzymes in maize identified by yeast two-hybrid screening. Physiol Plant **125:** 141–156

**Igamberdiev AU, Hurry V, Kromer S, Gardestrom P** (1998) The role of mitochondrial electron transport during photosynthetic induction. A

study with barley (Hordeum vulgare) protoplasts incubated with rotenone and oligomycin. Physiol Plant **104:** 431–439

**Iglesias AA, Vicario LR, Gómez-Casati DF, Sesma JI, Gómez-Casati ME, Bustos DM, Podestá FE** (2002) On the interaction of substrate analogues with non-phosphorylating glyceraldehydes 3-phosphate dehydrogenase from celery leaves. Plant Sci **162:** 689–696

**Kelly GJ, Gibbs M** (1973a) A mechanism for the indirect transfer of photosynthetically reduced nicotinamide adenine dinucleotide phosphate from chloroplasts to the cytoplasm. Plant Physiol **52:** 674–676

**Kelly GJ, Gibbs M** (1973b) Nonreversible d-glyceraldehyde 3-phosphate dehydrogenase of plant tissues. Plant Physiol **52:** 111–118

**Koksharova O, Schubert M, Shestakov S, Cerff R** (1998) Genetic and biochemical evidence for distinct key functions of two highly divergent GAPDH genes in catabolic and anabolic carbon flow of the cyanobacterium Synechocystis sp. PCC 6803. Plant Mol Biol **36:** 183–194

**Li J, Kogan M, Knight SA, Pain D, Dancis A** (1999) Yeast mitochondrial protein, Nfs1p, coordinately regulates iron-sulfur cluster proteins, cellular iron uptake, and iron distribution. J Biol Chem **274:** 33025–33034

**Mateos ML, Serrano A** (1992) Occurrence of phosphorylating and non-phosphorylating NADP+-dependent gylceraldehyde 3-phosphate dehydrogenases in photosynthetic organisms. Plant Sci **84:** 163–170

**Michels S, Scagliarini S, Della Seta F, Carles C, Riva M, Trost P, Branlant G** (1994) Arguments against a close relationship between non-phosphorylating and phosphorylating glyceraldehyde-3-phosphate dehydrogenases. FEBS Lett **339:** 97–100

**Millar AH, Considine MJ, Day DA, Whelan J** (2001) Unravelling the role of mitochondria during oxidative stress in plants. IUBMB Life **51:** 201–205

**Moller IM** (2001) Plant mitochondria and oxidative stress: electron transport, NADPH turnover, and metabolism of reactive oxygen species. Annu Rev Plant Physiol Plant Mol Biol **52:** 561–591

**Moller IM, Kristensen BK** (2004) Protein oxidation in plant mitochondria as a stress indicator. Photochem Photobiol Sci **3:** 730–735

**Nagata T, Todoriki S, Hayashi T, Shibata Y, Mori M, Kanegae H, Kikuchi S** (1999) Gamma-radiation induces leaf trichome formation in Arabidopsis. Plant Physiol **120:** 113–120

**Perusse JR, Schoen DJ** (2004) Molecular evolution of the GapC gene family in Amsinckia spectabilis populations that differ in outcrossing rate. J Mol Evol **59:** 427–436

**Petersen J, Brinkmann H, Cerff R** (2003) Origin, evolution, and metabolic role of a novel glycolytic GAPDH enzyme recruited by land plant plastids. J Mol Evol **57:** 16–26

**Pietrzak M, Shillito RD, Hohn T, Potrykus I** (1986) Expression in plants of two bacterial antibiotic resistance genes after protoplast transformation with a new plant expression vector. Nucleic Acids Res **14:** 5857–5868

**Plaxton WC** (1989) Molecular and immunological characterization of plastid and cytosolic pyruvate kinase isozymes from castor oil endosperm and leaf. Eur J Biochem **181:** 443–451

**Plaxton WC** (1996) The organization and regulation of plant glycolysis. Annu Rev Plant Physiol Plant Mol Biol **47:** 185–214

**Plaxton WC, Podestá FE** (2006) The functional organization and control of plant respiration. Crit Rev Plant Sci **25:** 159–198

**Rius SP, Casati P, Iglesias AA, Gomez-Casati DF** (2006) Characterization of an Arabidopsis thaliana mutant lacking a cytosolic non-phosphorylating glyceraldehyde-3-phosphate dehydrogenase. Plant Mol Biol **61:** 945–957

**Rumpho ME, Edwards GE, Loescher WH** (1983) A pathway for photosynthetic carbon flow to mannitol in celery leaves: activity and localization of key enzymes. Plant Physiol **73:** 869–873

**Russell DA, Sachs MM** (1989) Differential expression and sequence analysis of the maize glyceraldehyde-3-phosphate dehydrogenase gene family. Plant Cell **1:** 793–803

**Salt DE, Prince RC, Pickering IJ, Raskin I** (1995) Mechanisms of cadmium mobility and accumulation in Indian mustard. Plant Physiol **109:** 1427–1433

**Sambrook J, Maniatis T, Fritsch EF** (1989) Molecular Cloning: A Laboratory Manual, Ed 2. Cold Spring Harbor Laboratory, Cold Spring Harbor, NY

**Schnurr JA, Storey KK, Jung HJ, Somers DA, Gronwald JW** (2006) UDP-sugar pyrophosphorylase is essential for pollen development in Arabidopsis. Planta **224:** 520–532

**Siddiquee KA, Arauzo-Bravo MJ, Shimizu K** (2004) Effect of a pyruvate kinase (pykF-gene) knockout mutation on the control of gene expression and metabolic fluxes in Escherichia coli. FEMS Microbiol Lett **235:** 25–33

**Sparla F, Fermani S, Falini G, Zaffagnini M, Ripamonti A, Sabatino P, Pupillo P, Trost P** (2004) Coenzyme site-directed mutants of photosynthetic A4-GAPDH show selectively reduced NADPH-dependent catalysis, similar to regulatory AB-GAPDH inhibited by oxidized thioredoxin. J Mol Biol **340:** 1025–1037

**Sweetlove LJ, Heazlewood JL, Herald V, Holtzapffel R, Day DA, Leaver CJ, Millar AH** (2002) The impact of oxidative stress on Arabidopsis mitochondria. Plant J **32:** 891–904

**Tusher V, Tibshirani R, Chu G** (2001) Significance analysis of microarrays applied to the ionizing radiation response. Proc Natl Acad Sci USA **98:** 5116–5121

**Valverde F, Ortega JM, Losada M, Serrano A** (2005) Sugar-mediated transcriptional regulation of the Gap gene system and concerted photosystem II functional modulation in the microalga Scenedesmus vacuolatus. Planta **221:** 937–952

**Wang X, Chen Y, Zou J, Wu W** (2007) Involvement of a cytoplasmic glyceraldehyde-3-phosphate dehydrogenase GapC-2 in low-phosphate-induced anthocyanin accumulation in Arabidopsis. Chin Sci Bull **52:** 1764–1770

**Weigel D, Glazebrook J** (2006) Transformation of Agrobacterium using the freeze-thaw method. Cold Spring Harb Protoc doi/10.1101/pdb.prot4665

**Wolosiuk RA, Buchanan BB** (1978) Activation of chloroplast NADP-linked glyceraldehyde-3-phosphate dehydrogenase by the ferredoxin/thioredoxin system. Plant Physiol **61:** 669–671

**Wu P, Ma L, Hou X, Wang M, Wu Y, Liu F, Deng XW** (2003) Phosphate starvation triggers distinct alterations of genome expression in Arabidopsis roots and leaves. Plant Physiol **132:** 1260–1271

**Wulff K, Döppen W** (1985) Luminometric method. *In* HU Bergmeyer, ed, Methods of Enzymatic Analysis, Vol 7. Verlag Chemie, Weinheim, Germany, pp 357–364

**Yang Y, Kwon HB, Peng HP, Shih MC** (1993) Stress responses and metabolic regulation of glyceraldehyde-3-phosphate dehydrogenase genes in Arabidopsis. Plant Physiol **101:** 209–216